Title
A neural network that links brain function, white-matter structure and risky behavior

Authors
Kohno, Milky
Morales, Angelica M
Guttman, Zoe
et al.

Publication Date
2017-04-01

DOI
10.1016/j.neuroimage.2017.01.058

Peer reviewed

HHS Public Access

Author manuscript

Neuroimage. Author manuscript; available in PMC 2018 April 01.

Published in final edited form as:

Neuroimage. 2017 April 01; 149: 15–22. doi:10.1016/j.neuroimage.2017.01.058.

A neural network that links brain function, white-matter structure and risky behavior

Milky Kohno[a,*], **Angelica M. Morales**[a,*], **Zoe Guttman**[b], and **Edythe D. London, PhD**[a,b,c,d]

[a]Dept. of Psychiatry & Biobehavioral Sciences, University of California Los Angeles, Los Angeles, CA 90095, USA

[b]Neuroscience Interdepartmental Program, University of California Los Angeles, Los Angeles, CA 90095, USA

[c]Dept. of Molecular & Medical Pharmacology, University of California Los Angeles, Los Angeles, CA 90095, USA

[d]Brain Research Institute, University of California Los Angeles, Los Angeles, CA 90095, USA

Abstract

The ability to evaluate the balance between risk and reward and to adjust behavior accordingly is fundamental to adaptive decision-making. Although brain-imaging studies consistently have shown involvement of the dorsolateral prefrontal cortex, anterior insula and striatum during risky decision-making, activation in a neural network formed by these regions has not been linked to structural connectivity. Therefore, in this study, white-matter connectivity was measured with diffusion-weighted imaging in 40 healthy research participants who performed the Balloon Analogue Risk Task, a test of risky decision-making, during fMRI. Fractional anisotropy within a network that includes white-matter pathways connecting four regions (the prefrontal cortex, insula and midbrain to the striatum) was positively correlated with the number of risky choices and total amount earned on the task, and with the parametric modulation of activation in regions within the network to the level of risk during choice selection. Furthermore, analysis using a mixed model demonstrated how relationships of the parametric modulation of activation in each of the four aforementioned regions are related to risk probabilities, and how previous trial outcomes and task progression influence the choice to take risk. The present findings provide the first direct evidence that white-matter integrity is linked to function within previously identified components of a network that is activated during risky decision-making, and demonstrate that the integrity of white-matter tracts is critical in consolidating and processing signals between cortical and striatal circuits during the decision-making process.

Keywords

Risky decision making; diffusion tensor imaging; functional magnetic resonance imaging

Corresponding Author: Edythe D. London, Ph.D. elondon@mednet.ucla.edu, Address: UCLA Semel Institute, 760 Westwood Plaza, Los Angeles, CA 90095, Phone: (310) 825-0606, Fax: (310) 825-0812.

*authors contributed equally to this work

Disclosure/Conflict of Interest

The investigators have no conflicts of interest or financial disclosures to report.

1. Introduction

Neuroimaging studies have shown that activation in the prefrontal cortex (PFC), striatum, and insula is important for maintaining the neural representations of risk and reward (Paulus et al., 2003; Kuhnen and Knutson, 2005; Rao et al., 2008; Kohno et al., 2013), but how structural connectivity between these brain regions influences risky decision-making and associated neural function is unclear. Activity in the insula is associated with tracking risk (Ishii et al., 2012; Naqvi et al., 2014; Paulus et al., 2003; Kuhnen and Knutson, 2005), and patients with insula lesions make choices that reflect insensitivity to the odds of winning on gambling tasks (Clark et al., 2008). In addition, projections from the midbrain to the striatum signal the presence of motivationally salient events, and anticipatory dopaminergic responses modulate risk preferences (St Onge and Floresco, 2009; Sugam et al., 2012). Afferents from the PFC to the striatum facilitate shifts in decision-making on the basis of reward contingencies in rodents (St Onge et al., 2012); and in humans, corticostriatal functional connectivity has been associated with right dorsolateral PFC (rDLPFC) function during risky decision-making (Kohno et al., 2014). Notably, anatomical studies of nonhuman primates have identified white-matter pathways that link the striatum with the PFC, insula and midbrain (Lynd-Balta and Haber, 1994). It is therefore plausible that structural connectivity between the striatum and these three regions may be critical for integrating the signals that shape adaptive decision-making.

Few studies have examined the association between white-matter integrity and risky decision-making. Impairments on the Iowa Gambling task are linked to lower fractional anisotropy (FA), an index of white-matter integrity, of the superior longitudinal fasciculus, corticospinal tract, and superior corona radiata in cocaine-dependent participants (Lane, Steinberg et al. 2010), and in frontal, parietal, occipital, and callosal regions across samples of healthy and alcohol-dependent participants (Zorlu et al., 2013). These studies have begun to detail the importance of white-matter integrity in reward-based risky decision-making, but the links between structural connectivity and functional brain activation have not been directly examined.

Relationships between structural connectivity and functional activity have been observed in studies combining diffusion tensor imaging (DTI) and functional magnetic resonance imaging (fMRI) (Bennett and Rypma, 2013), consistent with the view that brain function parallels structural connectivity. It was recently shown that coherence of a tract connecting the anterior insula and nucleus accumbens was correlated with reduced risk-taking, indexed by a participant's preference for positively-skewed gambles, and that this association was mediated by activation in the nucleus accumbens (Leong et al., 2016). The goal of the present study was to assess how structural connectivity within a broader network influences network-wide activation during risky decision-making.

Decision-making and neural activation were modeled using The Balloon Analogue Risk Task (BART) (Lejuez et al., 2002) paired with fMRI. During the BART, participants can pump a balloon for greater potential gain while risking the loss of accumulated earnings. In each trial, the alternate choice is to cash-out and retain earnings accrued. White-matter

pathways connecting the striatum to the rDLPFC and anterior insula were selected on the basis of previous findings that activation in these regions was parametrically modulated by levels of risk and reward on the BART (Kohno et al., 2013). In addition, two studies paired transcranial stimulation with the Risk Task (Rogers, Owen et al. 1999), showing that risky choices were influenced by stimulation of the rDLPFC. Specifically, risk-taking behavior was affected by repetitive transcranial magnetic stimulation over the right but not the left DLPFC (Knoch, Gianotti et al. 2006) and by anodal stimulation over the right DLPFC coupled with cathodal stimulation over the left DLPFC with no changes in behavior when anodal stimulation was applied to the left DLPFC coupled with cathodal stimulation over the right DLPFC (Rogers, Owen et al. 1999). Therefore, FA was determined in white-matter pathways connecting the striatum with the rDLPFC, anterior insula and midbrain.

Previous studies have shown that poor decision-making on the Gambling Task, a test in which risk-taking leads to a smaller amount of earnings, is negatively associated with FA in white-matter tracts (Lane, Steinberg et al. 2010), but taking more risk as the trials progress on the BART is an adaptive strategy that produces a more positive outcome (Dean, Sugar et al. 2011). In addition, resting-state functional connectivity between the rDLPFC and striatum is positively related to the sensitivity of rDLPFC activation to levels of risk during decision-making (Kohno et al., 2014), and rDLPFC function is positively associated with overall performance (Kohno et al., 2013). Given these findings it was expected that FA would be positively associated with the modulation of activation in the rDLPFC, striatum and insula by risk.

2. METHODS

2.1 Participants

Forty healthy, right-handed research volunteers (18–51 years of age: mean= 27.83 SD= 1.79; 10 female) participated in this study, which was approved by the UCLA Office of the Human Research Protection Program. Each participant provided written informed consent prior to enrollment. Exclusion criteria, determined by a physical examination and psychiatric evaluation using the Structured Clinical Interview for DSM-IV, were: systemic, neurological, cardiovascular, or pulmonary disease; head trauma with loss of consciousness; any current Axis I psychiatric diagnoses except nicotine dependence; and current use of prescribed psychotropic medications. Participants who tested positive for cocaine, marijuana, methamphetamine, benzodiazepines, or opiates by urine toxicology were excluded, as were those with MRI contraindications.

2.2 Balloon Analog Risk Task

A version of the BART (Lejuez et al., 2002), adapted for event-related fMRI, was used (Fig. 1). Red or blue balloons were presented on active trials, and white balloons were presented on control trials. Participants were instructed that when an active balloon was presented, they should choose between pumping the balloon for a potential increase in earnings ($0.25/pump) or cashing out to retain the earnings accumulated during that trial. Either choice was registered by a bar press. Pumping increased the size of an active balloon and accumulated earnings, or resulted in the balloon exploding and forfeiture of unrealized earnings

accumulated during the trial. Trials included all pumps starting with the first presentation of a balloon and ended with the choice to cash out, which resulted in a 2-s display of the total earned or in a balloon explosion followed by a 2-s display of an exploded balloon with the message, “Total=$ 0.00”. Prior to scanning, participants were informed that red and blue balloons were associated with monetary reward and that they would receive their winnings after scanning, but not that the number of pumps to produce an explosion was pre-determined. For each active balloon trial, that number was determined from a uniform probability distribution, ranging from 1 to 8 and 1 to 12 pumps for red and blue balloons, respectively. Participants were informed that the white balloons did not explode and were not associated with potential reward, and that they should pump each white balloon until the trial ended. The white balloon trials were used to control for activation related to motor activity and visual processing. The number of white-balloon presentations within the trial varied randomly between 1–12, according to a uniform distribution. Red, blue and white balloon trials were randomly interspersed throughout the task. The task was administered in two 10-min runs. Because the task was self-paced and each balloon remained on the screen until the participant pressed a button, the total number of trials varied with the participant. Participants were able to cash out at any time prior to a balloon explosion, and the number of pumps within a trial depended on the participant’s choices. Participants could also avoid pumping the first balloon and choose to cash-out and receive $ 0.25. The inter-stimulus interval for balloon presentations was randomly sampled from a uniform distribution ranging from 1–3 s, and the inter-trial interval was randomly sampled from an exponential distribution (mean: 4 s; range: 1–14 s). Participants received their earnings in cash at the end of the scanning session.

2.3 fMRI Acquisition

Imaging was performed at 3 Tesla on a Siemens Magnetom Trio MRI system. A set of 302 functional, T2*-weighted, echoplanar images (EPI) were acquired (slice thickness = 4 mm; 34 slices; repetition time = 2 s; echo time = 30 ms; flip angle = 90°; matrix = 64 × 64; field of view = 200 mm). High-resolution, T2-weighted, matched-bandwidth and magnetization-prepared rapid-acquisition gradient echo (MPRAGE) scans were also acquired using an oblique axial orientation to maximize brain coverage and to optimize signal from ventromedial prefrontal regions.

2.4 DTI Acquisition

DTI data were acquired on a 3T Trio Scanner at a resolution of $2 \times 2 \times 2$ mm^3 (TR=8400 ms; TE=93 ms). One volume had no diffusion weighting (b=0), and diffusion gradients were applied along 64 directions at a diffusion weighting of b=1000.

2.5 Analysis of fMRI Data

Image analysis was performed using the FMRIB Software Library (FSL; version 5.0; www.fmrib.ox.ac.uk/fsl). The image series from each participant was first realigned to compensate for small head movements (Jenkinson et al., 2002), and then high-pass temporal filtering (100-sec) was applied. Data were spatially smoothed using a 5-mm FWHM Gaussian kernel, and skull-stripping was performed using the FSL Brain Extraction Tool. EPI images were first registered to the matched-bandwidth structural image, then to the

high-resolution MPRAGE structural image, and finally into standard Montreal Neurological Institute space, using 12-parameter affine transformations. Registration of MPRAGE structural images to standard space was further refined using FNIRT nonlinear registration (Andersson et al., 2007). Statistical analyses were performed on data in native space using FMRIBs fMRI Expert Analysis Tool (FEAT), and the statistical maps were spatially normalized to standard space prior to higher-level analysis.

Four types of events were included in the general linear model (GLM): pumps on active balloons, cash outs, balloon explosions and pumps on control balloons. Active-balloon and control-balloon pump events were defined as starting with the onset of the balloon presentation and ending with the button press to pump. Cash-out events were defined as the time between the appearance of the balloon and the disappearance of the feedback message, displaying the total earned. The balloon explosion event started with the appearance of and ended with the disappearance of the image of the exploded balloon and the message "Total Earned = $0.00". As a trial progressed, risk and potential reward increased with each pump, as did the amount earned with the choice to cash out. For each of the four types of events, estimates of mean activation and of parametric modulation of activation by pump number were included in a GLM using FEAT. Parametric regressors tested the linear relationship between pump number and blood oxygen level dependent (BOLD) signal, by using demeaned pump number (pump number minus mean number of pumps within each trial) as a parametric modulator with greater weight assigned to later pumps. For example, within a trial, the second pump event, for which twice the reward was at stake, was given twice the weight as the first. The parametric modulator for cash-out and explode events was the number of pumps before the decision to cash out or before the balloon exploded, respectively. The nonparametric regressors were used to estimate the mean response for each event without consideration of the escalation of potential reward/loss within the trial.

Regressors were created by convolving a set of *delta* functions that represented the onset times of the events with a canonical (double-*gamma*) hemodynamic response function (HRF). The participant's response time to pump and the inter-stimulus interval determined the width of the HRF for each event. In order for the HRF to approach baseline prior to the cash-out or balloon-explosion event, the width of the HRF for the last pump of each trial was modeled using the participant's response time. Additional regressors that represented the first temporal derivatives of the eight event-related regressors were included to capture variance associated with slight variations in the temporal lag of the hemodynamic response.

Whole-brain statistical analyses, using a fixed-effects model, were conducted separately for each imaging run per participant, and again to combine contrast images across the two runs. For between-participant analyses, the FMRIB Local Analysis of Mixed Effects module was used with sex and age as covariates. Thresholds for statistical images were set at a voxel height of $Z > 2.3$ and a cluster-probability threshold of $p < 0.05$, corrected for whole-brain multiple comparisons using the Theory of Gaussian Random Fields.

2.6 DTI Preprocessing

DTI data were preprocessed using the diffusion toolbox in FSL (http://fsl.fmrib.ox.ac.uk/fsl/fsl-4.1.9/fdt/index.html). Images were first corrected for motion and eddy currents. A

diffusion tensor model was fit at each voxel, and whole-brain maps of FA were generated. Voxelwise estimates of the angular distribution of local tract direction were calculated using BedpostX, which estimated a 2-fiber model using Markov Chain Monte Carlo sampling. A region of interest (ROI) sampling the midbrain, encompassing the ventral tegmental area and the substantia nigra, was hand-drawn on a standard template. The striatum was defined as indicated in the Harvard-Oxford Atlases, and the region of prefrontal cortex sampled was the middle frontal gyrus (MFG), as defined in the Desikan–Killiany Atlas (Desikan et al., 2006). Considering previous studies that parcellated the insula on the basis of function (Deen et al., 2011), the anterior and posterior components of the insula were separated along the left/right plane of the anterior commissure (MNI coordinate: Y=4) (Morales et al., 2014). ProbtrackX was used to determine the probability of connectivity between the striatum and midbrain, striatum and MFG, and striatum and anterior insula. Each tract was delineated twice, once with the striatum as a seed and the midbrain, striatum or MFG as termination/waypoint masks and vice versa. For every voxel in the seed mask, Probtrackx sampled from the posterior distribution of fiber orientations and computed a streamline through local fiber samples. Five thousand streamlines were traced from every voxel in the seed mask, and voxel values in the resulting maps represented the number of streamlines that entered that voxel when tracing between the seed and the termination/waypoint mask (where tracing ceased). The two maps for each tract were added together, transformed to standard space using FNIRT, and were binarized and averaged. Then a threshold of 0.8 was applied to remove any voxels that did not have streamlines connecting the seed and target masks in at least 80% of the participants (Fig. 2).

Tract-based spatial statistics (TBSS) was used to register individual FA maps into standard space using a nonlinear registration algorithm. FA maps were averaged across all subjects, and the resulting average was thinned to create a registration-invariant average FA “skeleton.” A threshold of 0.2 was applied to the average FA skeleton to remove areas with low FA or high inter-subject variability. FA values for each subject were then projected onto the skeleton from the nearest tract center. Masks of pathways between the seed and target mask generated with Probtrackx were used to extract average values from the FA skeleton.

2.7 Analysis of fMRI, DTI and Behavior

A Mixed Effects (FLAME1) module (Beckmann et al., 2003) was used for between-participant data analyses. The average FA of white-matter tracts connecting the striatum with the midbrain, insula and MFG, was taken as the measure for “network FA”, and was used as a regressor in group-level analyses. Statistical images were created using cluster-corrected statistics with a height threshold of $Z > 2.3$ and a cluster probability threshold of $p < 0.05$.

Two measures were calculated to represent overall task performance: total earnings and total number of pumps on trials that did not end in a balloon explosion. These values were used as outcome variables in partial correlation analyses with network FA and age, sex and smoking status as covariates. Post hoc tests of correlation between total earnings and total adjusted pumps with tracts connecting the striatum with the midbrain, insula, and MFG were performed using SPSS v22.

A general linear mixed model was used to test for relationships between brain function and risk-taking behavior. In the model, risk-taking behavior was indexed by pumps per trial. As trials progressed, risk-taking behavior may reflect exploring and learning the risk probabilities associated with balloon explosions; therefore, trial number (continuing across the two fMRI runs) and balloon color (red vs. blue balloons) were included in the model. In addition, the outcomes of each trial and the preceding trial were included to allow for an examination of the influence of explosions or the decision to cash-out on behavior (pumps). The model also included parameter estimates (β-values that corresponded to the modulation of activation by pump number) from regions where modulation of activation by pump number was associated with network FA in the whole-brain voxel-wise analysis. The rDLPFC was sampled as a spherical VOI with a 10-mm radius around the *peak* voxel (MNI coordinates: x=30, y=36, z=20) from a cluster that previously showed modulation of activation by risk during decision-making on the BART (Kohno et al., 2013). Bilateral caudate, putamen and nucleus accumbens regions were anatomically derived from the Harvard-Oxford subcortical atlas and were combined to create a VOI representing the whole striatum (left and right combined). The caudal anterior cingulate was anatomically defined using the Desikan-Killiany Atlas (Desikan et al., 2006), and the anterior insula was defined using information from a functional parcellation study (Deen et al., 2011). Also included in the model were the age, sex and smoking status of each participant.

3. RESULTS

3.1 fMRI during the BART

As reported previously (Kohno et al., 2013), pump number modulated activation in the right inferior and right middle frontal gyri, right orbitofrontal cortex, right insula, anterior cingulate, thalamus and brainstem ($p < 0.05$, whole-brain corrected) (data not shown).

3.2 fMRI and DTI Associations

Network FA was correlated with the parametric modulation of activation bilaterally in the anterior insula, putamen, anterior cingulate cortex (ACC) and right MFG ($p < 0.05$, whole-brain corrected) by risk (Fig. 3, Table 1). The effect size maps show how each tract contributes to the modulation of activation by level of risk in the rDLPFC, striatum, ACC and insula (Fig. 4). Tracts that connect the insula and striatum show the smallest effects on the modulation of activation, while the tracts connecting the midbrain and striatum have the largest effect on the modulation of activation in the rDLPFC, striatum, ACC and insula.

3.3 DTI and Behavioral Performance (Table 2)

Network FA was correlated with total adjusted pumps ($r = 0.297$, $p = 0.037$) and total earnings ($r = 0.299$, $p = 0.036$). FA in tracts connecting the midbrain with the striatum was correlated with total earnings ($r = 0.288$, $p = 0.042$) and showed a nonsignificant trend for positive association with total adjusted pumps ($r = 0.254$, $p = 0.064$). There were no significant relationships between FA in tracts connecting the MFG and the striatum with total adjusted pumps ($r = 0.059$, $p = 0.363$) or with total earnings ($r = 0.141$, $p = 0.202$). FA between the insula and striatum was associated with both total adjusted pumps ($r = 0.347$, $p = 0.018$) and total earnings ($r = 0.287$, $p = 0.042$).

3.4 fMRI and Performance on the BART (Table 3)

The parametric modulation of activation in the ACC ($F(1, 1,737) = 7.984$, $p = 0.005$) and whole striatum ($F(1, 1,738) = 6.444$, $p = 0.011$) to level of risk during decision-making interacted with the outcome of the previous trial to influence choice selection. Following a cashout, modulation of activation in the ACC and striatum was more negatively associated with risk level and number of pumps than on trials following a balloon explosion. Trial number also interacted with modulation of activation in the ACC ($F(1, 1,737) = 7.984$, $p = 0.005$) and whole striatum ($F(1, 1,738) = 6.444$, $p = 0.011$) on risk-taking, as indicated by number of pumps in a trial. Specifically, as trials progressed, participants decided to pump less when there was less modulation of ACC and striatal activation. There was a significant interaction of the parametric modulation of rDLPFC activation with outcome of an individual trial on choice selection ($F(1, 1,735) = 4.991$, $p = 0.026$); modulation of rDLPFC activation was positively associated with number of pumps before cashing out. There were no significant interactions of modulation of insula activation by risk with the trial-by-trial parameters on choice selection.

4. DISCUSSION

This study provides evidence that the structural integrity of a network comprising white-matter pathways connecting the prefrontal cortex, insula and midbrain to the striatum is related to network-wide brain function during risky decision-making and to risk-taking behavior, and indicates how different contextual factors interact with brain function to guide choice selection. By delineating a network that links brain function, white-matter integrity and risk-taking behavior, these results extend the observation that FA in the pathway connecting the insula to the nucleus accumbens is associated with activation in the nucleus accumbens and with risk taking (Leong et al., 2016). The present findings also detail how each tract independently is related to brain function.

Behavioral measures, specifically the choice to take risk and total earnings, were significantly associated with FA of the network, demonstrating the importance of white-matter integrity to brain function during risky-decision-making. As risk-taking on the BART is an adaptive strategy (Dean, Sugar et al. 2011), the positive relationship between FA and behavior is in line with studies showing that FA in the corona radiata, which connects DLPFC, ACC and the insula is negatively associated with impaired performance on the Iowa Gambling Task (Lane, Steinberg et al. 2010). FA in tracts connecting the insula and striatum was positively related to risk-taking, indicated by the number of choices to pump and the total earnings. These findings are in line with previous findings that the connectivity between anterior insula to nucleus accumbens correlates with inconsistent risk preferences indexed by the reduced tendency to choose positively skewed gambles (Leong, Pestilli et al. 2016) and that the insula provides a risk-prediction signal that guides risky choices (Preuschoff et al., 2008). FA in a tract between the midbrain and striatum was also positively associated with total earnings. Taken together, these results suggest that adaptive decision-making requires a balance in signaling, whereby white-matter tracts connecting the midbrain and striatum mediate signaling of potential reward while connections of the striatum with the insula have been implicated in the integration of value and risk representations.

Surprisingly, FA of white matter between the MFG and striatum was not correlated with risk-taking behavior or total earnings. Since DTI-derived indices of white-matter connectivity provide no information on direction of signaling, it is not possible to distinguish between the effects of “top-down” from “bottom-up” connections between the PFC and striatum. However, inclusion of these tracts in whole network FA improves the strength of the correlation with performance compared to the association with independent tracts, suggesting that white-matter pathways between the MFG and striatum do contribute to overall performance.

Results from this study extend previous findings that risky decision-making is associated with activation in the rDLPFC, anterior insula, striatum and ACC (Rao et al., 2008; Kohno et al., 2013), demonstrating an importance of structural integrity of white matter tracts to the parametric modulation of activation in these regions to risk. In addition, results of the mixed model analysis highlight the importance of each region within a network that integrates the various situational factors determining risky decision-making.

The association between the parametric modulation of ACC activation to risk and risk-taking behavior varied with the number of trials completed and the outcome of the previous trial is in line with a role of the ACC in error and performance monitoring (Paulus et al., 2002; Brown and Braver, 2008), and suggests that the parametric modulation of activation in the ACC may serve as a signal that maintains representations of task duration and recent gains to modify behavior (Brown, 2013). Similarly, the outcome of the previous trial and the trial number interacted with the parametric modulation of activation to risk in the whole striatum in influencing choice selection. This result is consistent with previous findings that striatal activation and striatal D2/D3 receptor availability were negatively correlated with number of pumps following a reward (Kohno et al., 2013), and suggests that striatal signaling modifies risk-taking behavior as a function of reward contingencies. In trials where participants decided to cash out, modulation of rDLPFC activation was positively associated with number of pumps, consistent with the role of the rDLPFC in maintaining goal-directed behavior (Miller and Cohen, 2001).

FA is influenced by a number of biological variables, such as myelination, axon caliber, and axon coherence (Beaulieu, 2009); therefore, greater FA may enhance signal transduction within and between cortical and striatal circuits. These results show that decision-making is, in part, a reflection of recent experiences and outcomes, which are represented and integrated by different regions within a functional network, and that therefore, the speed of signal transduction within that network is a critical variable in dynamic processing of factors that influence decision-making. As human and animal studies have indicated that signaling between the midbrain, striatum and prefrontal cortex mediates executive functions, including cognitive control, risk-taking, and impulsivity (Redgrave et al., 1999; Salamone and Correa, 2002), these findings suggest that structural connectivity of a mesolimbic/mesocortical network may be a key factor in integrating multiple synaptic inputs and in prescribing a balance between cortical and striatal regions to guide risky decision-making.

This study broadens our understanding of the neural networks important for risky decision-making, but has some limitations. The combination of the temporal resolution of fMRI with

the BART was not sufficient to allow for clear dissociation between the decision to cash out and the receipt of reward. In addition, because the magnitude of potential earnings as well as the risk of forfeiting earnings increased with each pump, it was not possible to separate the effects of risk from those of potential reward in modulation of cortical activation. In addition, FA is influenced by a number of factors such as myelination, axon caliber, and axon coherence (Beaulieu, 2009), and it is not possible to know the contribution of each to the present findings. However, future studies examining differences in axial diffusivity and radial diffusivity will provide a better understanding of how different indices of white-matter affect brain function and behavior.

5. Conclusions

Where other studies have focused on specific white-matter pathways and brain regions associated with decision-making, this study focused on network-wide activation as a function of dynamic situational factors and white-matter structure within a network of regions that contribute to decision-making under uncertain, risky conditions. The results provide insights into the dynamic interactions between activation and white-matter integrity of this network, suggesting that for adaptive decision-making, activation of the rDLPFC facilitates adaptive risky choices, while the ACC and striatum maintain representations of recent experience. The results demonstrate that the integration of decision-making factors by cortical and subcortical regions may depend on white-matter integrity within a neural network associated with risky decision-making.

Acknowledgments

Funding

The research described here was funded in part by NIH grants P20 DA022539, R01 DA020726, a grant from Philip Morris USA, and endowments from the Thomas P. and Katherine K. Pike Chair in Addiction Studies and the Marjorie M. Greene Trust. M Kohno and A Morales were supported by training grant T32 DA 024635. None of the sponsors were involved with the design, collection, analysis or interpretation of data, writing the manuscript or the decision to submit the manuscript for publication.

References

Andersson J, Jenkinson M, Smith S. Non-linear registration, aka Spatial normalisation. FMRIB technical report. 2007

Beaulieu, C. Diffusion MRI: From Quantitative Measurement to In Vivo Neuroanatomy. Johansen-Berg, H., Behrens, TE., editors. London: Elsevier; 2009. p. 105-126.

Beckmann CF, Jenkinson M, Smith SM. General multilevel linear modeling for group analysis in FMRI. NeuroImage. 2003; 20:1052–1063. [PubMed: 14568475]

Bennett IJ, Rypma B. Advances in functional neuroanatomy: a review of combined DTI and fMRI studies in healthy younger and older adults. Neurosci Biobehav Rev. 2013; 37:1201–1210. [PubMed: 23628742]

Brown JW. Beyond conflict monitoring: Cognitive control and the neural basis of thinking before you act. Curr Dir Psychol Sci. 2013; 22:179–185. [PubMed: 25360064]

Brown JW, Braver TS. A computational model of risk, conflict, and individual difference effects in the anterior cingulate cortex. Brain Res. 2008; 1202:99–108. [PubMed: 17707352]

Clark L, Bechara A, Damasio H, Aitken MR, Sahakian BJ, Robbins TW. Differential effects of insular and ventromedial prefrontal cortex lesions on risky decision-making. Brain. 2008; 131:1311–1322. [PubMed: 18390562]

Dean AC, Sugar CA, Hellemann G, London ED. Is all risk bad? Young adult cigarette smokers fail to take adaptive risk in a laboratory decision-making test. Psychopharmacology (Berl). 2011; 215(4): 801–811. [PubMed: 21293849]

Deen B, Pitskel NB, Pelphrey KA. Three systems of insular functional connectivity identified with cluster analysis. Cereb Cortex. 2011; 21:1498–1506. [PubMed: 21097516]

Desikan RS, Segonne F, Fischl B, Quinn BT, Dickerson BC, Blacker D, Buckner RL, Dale AM, Maguire RP, Hyman BT, Albert MS, Killiany RJ. An automated labeling system for subdividing the human cerebral cortex on MRI scans into gyral based regions of interest. NeuroImage. 2006; 31:968–980. [PubMed: 16530430]

Ishii H, Ohara S, Tobler PN, Tsutsui K, Iijima T. Inactivating anterior insular cortex reduces risk taking. J Neurosci. 2012; 32:16031–16039. [PubMed: 23136439]

Jenkinson M, Bannister P, Brady M, Smith S. Improved optimization for the robust and accurate linear registration and motion correction of brain images. NeuroImage. 2002; 17:825–841. [PubMed: 12377157]

Knoch D, Gianotti LR, Pascual-Leone A, Treyer V, Regard M, Hohmann M, Brugger P. Disruption of right prefrontal cortex by low-frequency repetitive transcranial magnetic stimulation induces right-taking behavior. J Neurosci. 2006; 26:6469–6472. [PubMed: 16775134]

Kohno M, Morales AM, Ghahremani DG, Hellemann G, London ED. Risky decision making, prefrontal cortex, and mesocorticolimbic functional connectivity in methamphetamine dependence. JAMA Psychiatry. 2014; 71:812–820. [PubMed: 24850532]

Kohno M, Ghahremani DG, Morales AM, Robertson CL, Ishibashi K, Morgan AT, Mandelkern MA, London ED. Risk-Taking Behavior: Dopamine D2/D3 Receptors, Feedback, and Frontolimbic Activity. Cereb Cortex. 2013

Kuhnen CM, Knutson B. The Neural Basis of Financial Risk Taking. Neuron. 2005; 47:763–770. [PubMed: 16129404]

Lane SD, Steinberg JL, Ma L, Hasan KM, Kramer LA, Zuniga EA, Narayana PA, Moeller FG. Diffusion tensor imaging and decision making in cocaine dependence. PLoS One. 2010; 5(7):e11591. [PubMed: 20661285]

Lejuez CW, Read JP, Kahler CW, Richards JB, Ramsey SE, Stuart GL, Strong DR, Brown RA. Evaluation of a behavioral measure of risk taking: the Balloon Analogue Risk Task (BART). J Exp Psychol Appl. 2002; 8:75–84. [PubMed: 12075692]

Leong JK, Pestilli F, Wu CC, Samanez-Larkin GR, Knutson B. White-Matter Tract Connecting Anterior Insula to Nucleus Accumbens Correlates with Reduced Preference for Positively Skewed Gambles. Neuron. 2016; 89:63–69. [PubMed: 26748088]

Lynd-Balta E, Haber SN. The organization of midbrain projections to the striatum in the primate: sensorimotor-related striatum versus ventral striatum. Neuroscience. 1994; 59:625–640. [PubMed: 7516506]

Miller EK, Cohen JD. An integrative theory of prefrontal cortex function. Annu Rev Neurosci. 2001; 24:167–202. [PubMed: 11283309]

Morales AM, Ghahremani D, Kohno M, Hellemann GS, London ED. Cigarette exposure, dependence, and craving are related to insula thickness in young adult smokers. Neuropsychopharmacology. 2014; 39:1816–1822. [PubMed: 24584328]

Naqvi NH, Gaznick N, Tranel D, Bechara A. The insula: a critical neural substrate for craving and drug seeking under conflict and risk. Ann N Y Acad Sci. 2014; 1316:53–70. [PubMed: 24690001]

Paulus MP, Hozack N, Frank L, Brown GG. Error rate and outcome predictability affect neural activation in prefrontal cortex and anterior cingulate during decision-making. NeuroImage. 2002; 15:836–846. [PubMed: 11906224]

Paulus MP, Rogalsky C, Simmons A, Feinstein JS, Stein MB. Increased activation in the right insula during risk-taking decision making is related to harm avoidance and neuroticism. NeuroImage. 2003; 19:1439–1448. [PubMed: 12948701]

Preuschoff K, Quartz SR, Bossaerts P. Human insula activation reflects risk prediction errors as well as risk. J Neurosci. 2008; 28:2745–2752. [PubMed: 18337404]

Rao H, Korczykowski M, Pluta J, Hoang A, Detre JA. Neural correlates of voluntary and involuntary risk taking in the human brain: An fMRI Study of the Balloon Analog Risk Rask (BART). NeuroImage. 2008; 42:902–910. [PubMed: 18582578]

Redgrave P, Prescott TJ, Gurney K. The basal ganglia: a vertebrate solution to the selection problem? Neuroscience. 1999; 89:1009–1023. [PubMed: 10362291]

Rogers RD, Owen AM, Middleton HC, Williams EJ, Pickard JD, Sahakian BJ, Robbins TW. Choosing between small, likely rewards and large, unlikely rewards activates inferior and orbital prefrontal cortex. J Neurosci. 1999; 19:9029–9038. [PubMed: 10516320]

Salamone JD, Correa M. Motivational views of reinforcement: implications for understanding the behavioral functions of nucleus accumbens dopamine. Behav Brain Res. 2002; 137:3–25. [PubMed: 12445713]

St Onge JR, Floresco SB. Dopaminergic modulation of risk-based decision making. Neuropsychopharmacology. 2009; 34:681–697. [PubMed: 18668030]

St Onge JR, Stopper CM, Zahm DS, Floresco SB. Separate prefrontal-subcortical circuits mediate different components of risk-based decision making. J Neurosci. 2012; 32:2886–2899. [PubMed: 22357871]

Sugam JA, Day JJ, Wightman RM, Carelli RM. Phasic nucleus accumbens dopamine encodes risk-based decision-making behavior. Biol Psychiatry. 2012; 71:199–205. [PubMed: 22055017]

Zorlu N, Gelal F, Kuserli A, Cenik E, Durmaz E, Saricicek A, Gulseren S. Abnormal white matter integrity and decision-making deficits in alcohol dependence. Psychiatry Res. 2013; 214:382–388. [PubMed: 24080516]

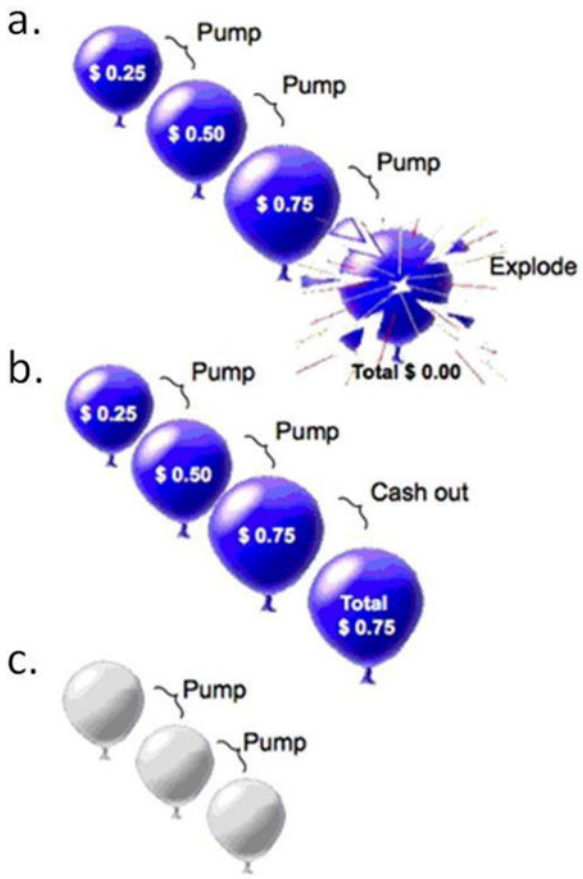

Figure 1. Balloon Analogue Risk Task

a. Pumping an active balloon increases potential earnings but carries risk of balloon explosion and loss of earnings accumulated during the trial. b. If participants cash out before the balloon explodes, they retain the earnings accumulated. c. White balloons, which do not increase in size with pumping, do not explode, and are not associated with reward potential, are presented in control trials (see 2. Methods).

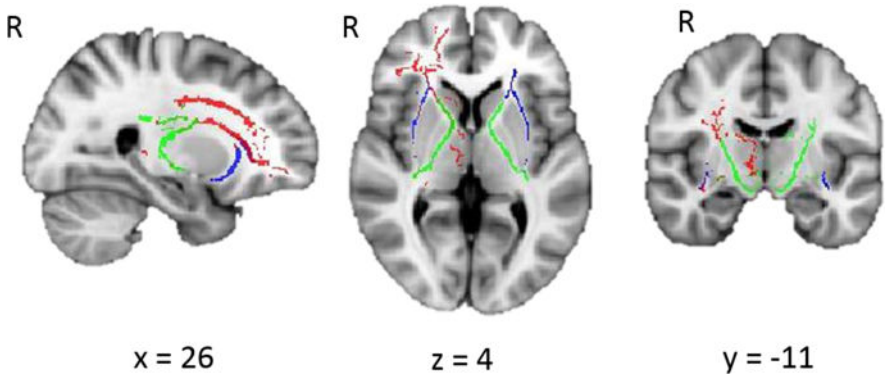

Figure 2. Structural connectivity within a network of regions involved in risky decision-making

Maps show TBSS derived white-matter skeleton in the pathways connecting the striatum with the right DLPFC (red), midbrain (green) and insula (blue). Fractional anisotropy (FA) was calculated by extracting data from each of these pathways and averaging the data to generate a single measure of white-matter integrity in a “risk-taking” network for each subject (n=40).

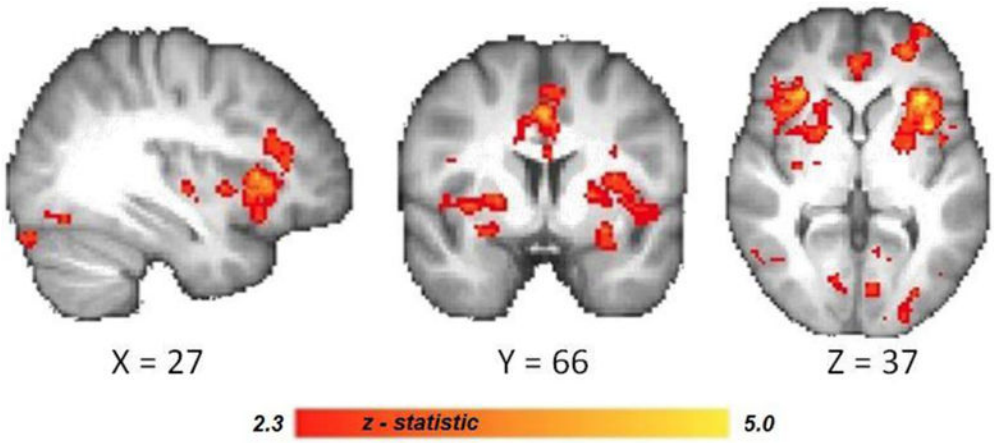

Figure 3. Positive relationship between fractional anisotropy within a network of regions involved in risky decision-making and the parametric modulation of activation to risk during risky decision-making

Statistical maps display regions where the parametric modulation of activation by levels of risk (indexed by pump number) is positively associated with fractional anisotropy within a network of regions activated during risky decision-making (X,Y,Z in voxel coordinates). Corrected for age, sex, smoking status and whole-brain multiple comparisons ($n = 40$, $p < 0.05$).

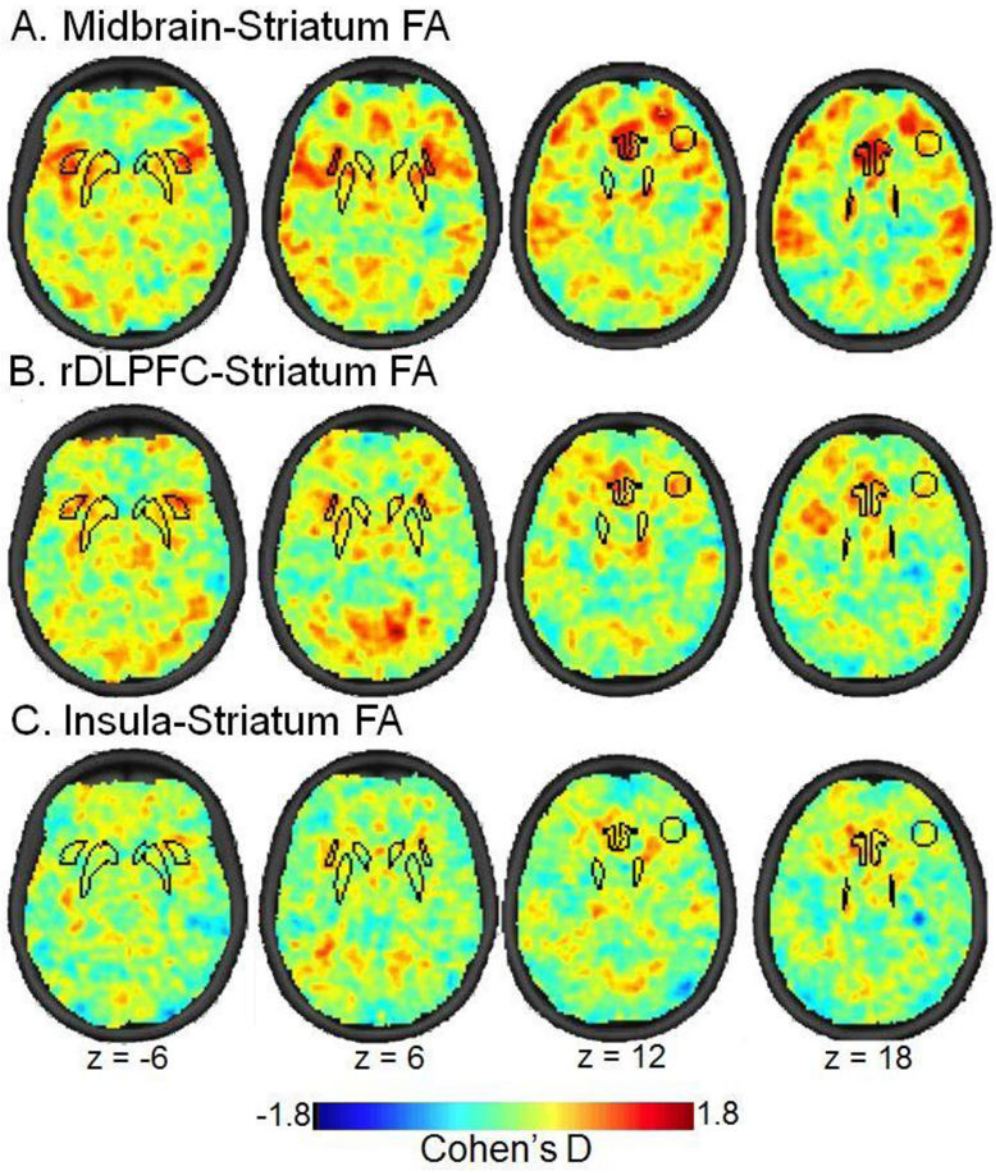

Figure 4. Maps depicting effect size for the association of structural connectivity with parametric modulation of brain activation to risk during risk taking

Warm colors (orange and red) depict brain regions showing positive association between the modulation of activation to levels of risk with fractional anisotropy in the pathways connecting the striatum with (A) the mibrain, (B) the right dorsolateral prefrontal cortex, and (C) the insula. Right hemisphere depicted on the right side of the image.

Table 1

Brain regions where network FA was associated with the parametric modulation of activation to levels of risk[a]

Brain region	Cluster size (voxels)	x [b]	y	z	Z statistic
Cluster #1	1171				
Anterior Cingulate Cortex		−2	30	20	3.92
Cluster #2	779				
Insula cortex (R)		32	26	4	3.72
Inferior frontal gyrus (R)		38	30	23	3.51
Middle frontal gyrus (R)		38	28	20	3.31
Putamen (R)					
Cluster #3	765				
Insula cortex (L)		−44	0	4	3.22
Putamen (L)		−38	6	8	3.15
Cluster #4	224				
Occipital Cortex		34	−84	16	3.09

[a] Amplitude of BOLD responses associated with pumps and cash outs on active balloons were modeled as a function of parametrically varied levels of risk and reward (represented by pump number) (see 2. Methods). Z-statistic maps were thresholded using cluster-corrected statistics with a height-threshold of $Z > 2.3$ and cluster-forming threshold of $p < 0.05$.

[b] x, y, z reflect coordinates for peak voxel or for other local maxima in MNI space.

Table 2

Associations between fractional anisotropy (FA) & Performance on the BART[a]

White Matter Pathway	Total Adjusted Pumps	Total Earnings
Striatum-Midbrain	r = .254, p = .064	r = .288, p = .042
Striatum-PFC	r = .059, p = .363	r = .141, p= .202
Striatum-Insula	r = .347, p = .018	r = .287, p= .042
"Risk-taking" Network [b]	r = .297, p = .037	r = .299, p = .036

[a] Partial correlations with age, sex, and smoking status as covariates, n = 40

[b] FA within the risk taking networks was calculated by averaging FA values derived from striatum-midbrain, striatum-PFC, and striatum-insula tracts.

Table 3

Mixed model interactions between task conditions and modulation of brain activation by risk and on pumping behavior[a]

Modulation of Activation	Balloon Type	Trial Number	Current Trial Outcome	Previous Trial Outcome
rDLPFC	F(1, 1,729) = 0.74 p = 0.390	F(1, 1,741) = .48 p = 0.491	F(1, 1,736) = 4.99 p = 0.026 *	F(1, 1,737) =2.47 p = 0.16
Striatum	F(1, 1,729) = 3.27 p = 0.071	F(1, 1,739) = 8.70 p = 0.003 *	F(1, 1,738) = 1.56 p = 0.213	F(1, 1,738) = 6.44 p = 0.011 *
ACC	F(1, 1,729) = 1.11 p = 0.292	F(1, 1,743) = 18.47 p = 0.000 *	F(1, 1,736) = 0.05 p = 0.817	F(1, 1,738) = 7.98 p = 0.005 *
Insula	F(1, 1,729) = 0.77 p = 0.380	F(1, 1,738) = 9.47 p = 0.002 *	F(1, 1,736) = 0.54 p = 0.464	F(1, 1,738) = 2.32 p = 0.128

[a]A mixed effects model was used to determine how parametric modulation of brain activation to pump number interacted with situational factors to impact the number of pumps per trial. The model also included age, sex and smoking status as fixed factors (n=40).